JOURNAL OF CATALYSIS 126, 361–369 (1990)

Interaction of 1-Butene and *n*-Butane with a Sulfate-Promoted Iron Oxide

JAE S. LEE,[1] MI H. YEOM, AND DOO S. PARK[2]

Department of Chemical Engineering, Pohang Institute of Science and Technology and Research Institute of Industrial Science and Technology, P.O. Box 125, Pohang, Korea

Received February 22, 1990; revised July 2, 1990

Interactions of sulfate-promoted iron oxide SO_4^{2-}–Fe_2O_3 with 1-butene and *n*-butane were investigated by means of infrared spectroscopy and temperature-programmed desorption/reaction coupled with mass spectrometry. By reacting with the sulfate ion, 1-butene adsorbed on SO_4^{2-}–Fe_2O_3 promoted sulfate decomposition. In contrast, adsorbed *n*-butane desorbed readily upon heating above 320 K. Implications of these findings in catalysis by this material are discussed.

INTRODUCTION

Sulfate-promoted iron oxide SO_4^{2-}–Fe_2O_3 is a superacid catalyst which can isomerize *n*-butane at room temperature (*1*). It has also been shown to exhibit pronounced catalytic activity for many acid-catalyzed reactions such as isomerization, dehydration, esterification, acylation, and hydrocracking (*2*). Our previous paper (*3*) described interactions of SO_4^{2-}–Fe_2O_3 with basic molecules such as pyridine and ammonia. These molecules upon adsorption at room temperature (RT) followed by heating, reacted with sulfate ion of SO_4^{2-}–Fe_2O_3 to promote its decomposition and removal from the surface. By means of infrared (IR) spectroscopy, the structure of a possible intermediate of the decomposition was proposed. The results are summarized in Fig. 1 for the case of pyridine as an example.

The SO_4^{2-}–Fe_2O_3 was proposed to assume a chelating bidentate structure I (*4*). The complex is characterized by a strong IR band near 1380 cm^{-1} due to the asymmetric vibration of S=O bond. Due to the induction effect of S=O in the sulfur complex, strong Lewis acid sites are generated on Fe. When a basic molecule such as pyridine adsorbs on the metal cation, the bond order of S=O is reduced from a highly covalent double bond character to a lesser double bond character as indicated by the reduced wave number of S=O group in species II. If the species II is heated, some of the adsorbed pyridine desorbs to regenerate the original species, but some pyridine react with the sulfate ion to form species III with S=O IR band at 1350 cm^{-1}. Upon further heating, this species decomposes to form low molecular weight gases such as SO_2 and CO_2, at a lower temperature than that for the thermal decomposition of SO_4^{2-}–Fe_2O_3 alone.

The present work takes a similar approach to investigate interactions of the surface sulfate group with 1-butene or *n*-butane. Skeletal isomerization of *n*-butane (*1*) and double bond isomerization of 1-butene (*5*) have been studied using SO_4^{2-}–Fe_2O_3 as a catalyst. Hence, understanding of these interactions could be important to understand the nature of catalytic reactions that involves this type of materials. As before (*3*), the temperature-programmed desorption/reaction (TPDR) and the IR spectroscopy are employed.

[1] To whom correspondence should be addressed.

[2] Present address: Cryogenic Research Institute, Dae Sung Sanso Co., Ltd., Ansan, Kyunggi, Korea.

0021-9517/90 $3.00

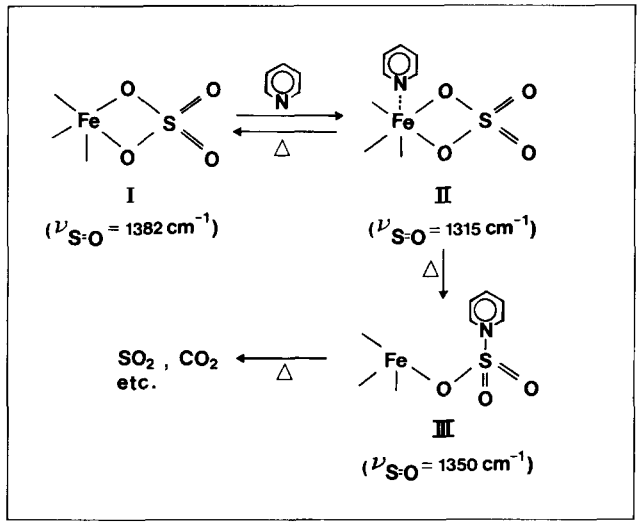

FIG. 1. Interactions between pyridine and SO_4^{2-}–Fe_2O_3.

EXPERIMENTAL

Experimental procedures similar to those described previously (*3*) were employed. Briefly, a SO_4^{2-}–Fe_2O_3 with 3.2 wt% of sulfur as SO_3 was prepared by immersing $Fe(OH)_3$ in an aqueous solution of $(NH_4)_2SO_4$ at 350 K and calcining the obtained precipitate at 770 K in air for 2.5 h. The $Fe(OH)_3$ was prepared by treating a 3 N aqueous solution of $Fe(NO_3)_3$ with 3 N aqueous ammonia, and then by washing and drying the product at 370 K for 24 h.

The TPDR was performed for a 100-mg powder sample evenly distributed on a coarse frits in a flow quartz cell. Before adsorption, the sample was treated for 2 h in He flowing at 86 μmol s^{-1} onto the sample maintained at 760 K. Adsorption of 1-butene or *n*-butane (both from Matheson, 99.0%) was performed by flowing an adsorbate onto the sample cooled to RT for 0.5 h. Series of liquid N_2, 4 Å molecular sieve, and MnO/SiO_2 traps were employed to purify He. The hydrocarbon adsorbates were used as received. After adsorption, the sample, still maintained at RT, was purged with He for 0.5 h to remove adsorbates in the gas phase and physisorbed on the sample. The temperature of the sample was raised at a linear rate of 0.33 K s^{-1}, in He flowing at 86 μmol s^{-1}. A furnace coupled to a controller/programmer heated the cell and a local thermocouple monitored the temperature of the sample. A thermowell containing the thermocouple was imbeded into the sample powder to ensure a good contact. Desorbed gases were analyzed by an on-line VG Micromass quadruple mass spectrometer (MS).

The IR measurements were made with a Perkin-Elmer 1800 FT–IR spectrometer on a self-supporting disk sample. The disk was prepared by compressing the powder under 6–8 $\times$ 10^3 kg cm^{-2} pressure and had a loading of 15–20 mg cm^{-2}. The IR cell was composed of two parts; the KBr window part to take IR spectra in the transmission mode and the sample treatment part. It could be connected to a flow system for sample treatments and transferred to the spectrometer without exposing the sample to the atmosphere. The adsorption and He purge were performed in the same manner as in TPDR experiments. The temperature of the sample was increased at a rate of 0.17 K s^{-1} to a desired temperature, and then rapidly cooled to RT to take an IR spectrum.

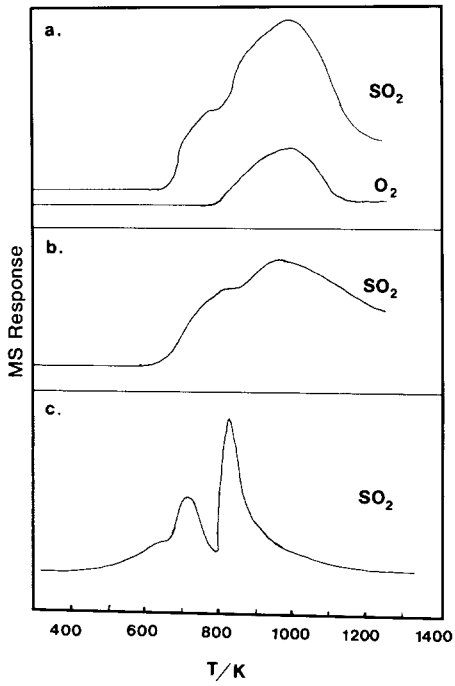

FIG. 2. The TPDR curves for fresh SO_4^{2-}–Fe_2O_3 (a) and SO_4^{2-}–Fe_2O_3 with preadsorbed butane (b), and 1-butene (c).

RESULTS

Temperature-Programmed Desorption and Reaction

When a SO_4^{2-}–Fe_2O_3 sample, without preadsorption, is subject to TPDR, it starts to decompose at 700 K to yield gaseous SO_2 (m/e = 64 or 48) and O_2 (m/e = 32), as indicated in Fig. 2a. The sulfate was mostly removed from the surface below 1200 K. The SO_2 TPDR showed roughly two peaks and the O_2 peak coincided with the second SO_2 peak. The SO_4^{2-}–Fe_2O_3 preadsorbed with *n*-butane showed TPDR spectra of SO_2 (Fig. 2b) and O_2 very similar to those without preadsorption.

In contrast to relatively simple TPDR patterns for samples without preadsorption and with *n*-butane, TPDR spectra for the sample with preadsorbed 1-butene were complicated. Figure 2c indicates that decomposition of the sulfate in this sample occurs at temperatures lower than those for the previous two cases. Furthermore, the shape of the spectrum is very different. A number of decomposition products other than SO_2 were detected as shown in Fig. 3. The other major components of TPDR were 1-butene (m/e = 56) and CO_2 (m/e = 44), and CH_4, O_2, H_2, and H_2O also were produced in relatively minor quantities. However, H_2S (m/e = 34) was not detected. It appears that 1-butene desorbs slightly above RT and the desorption is complete at 650 K. Formation of CO_2 with peaks at the same peak temperature of SO_2 formation suggests that two gases are produced from a common process occurring on the surface. Methane also was detected with the same peak temperature as for SO_2 and CO_2. Dioxygen which was the major component of the TPDR for the sample without adsorption or with *n*-butane showed only a signal so weak that it was difficult to locate the peak positions. For a blank experiment, 1-butene was flown into an empty cell and heated in the same manner. The H_2 formation from thermal decomposition of 1-butene was observed above 870 K. Hence, the effect of thermal decom-

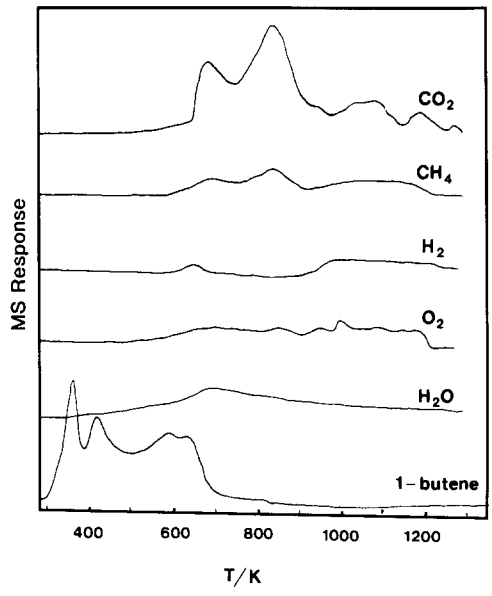

FIG. 3. The TPDR curves for SO_4^{2-}–Fe_2O_3 preadsorbed with 1-butene. For SO_2, see Fig. 2c.

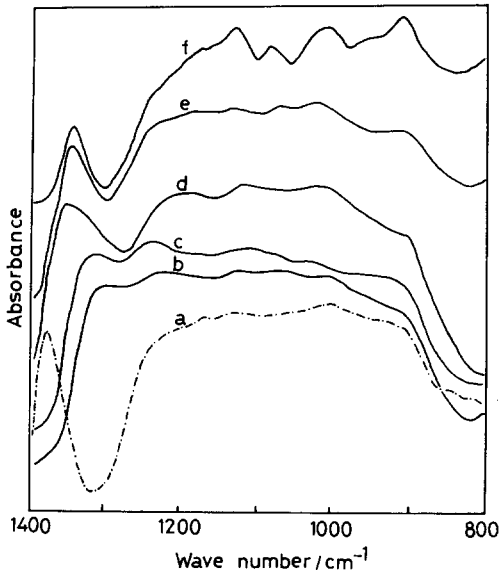

FIG. 4. Infrared spectra (800–1400 cm^{-1}) of SO_4^{2-}–Fe_2O_3 before and after adsorption of 1-butene. The fresh sample was treated at 760 K for 2 h in He flowing at 86 μmol s^{-1} (a). Following adsorption of 1-butene at RT, the sample was treated at RT (b), 420 K (c), 620 K (d), 670 K (e), and 720 K (f).

position could be excluded in most of the temperature range that showed significant TPDR features.

Infrared

The IR spectrum of SO_4^{2-}–Fe_2O_3 treated in He at 760 K for 2 h (Fig. 4a) shows the characteristic S=O band at 1382 cm^{-1} together with broad bands in 900–1250 cm^{-1}. This represents a typical spectrum of a well-prepared SO_4^{2-}–Fe_2O_3 with superacid character (*4*). Upon adsorption of 1-butene at RT, the sharp band disappears and new band appears near 1310 cm^{-1} (Fig. 4b). As the temperature of the sample with preadsorbed 1-butene is raised, this new band shifts to higher wave numbers and stands at 1350 cm^{-1} above 620 K.

Figure 5 shows three IR bands in 3000–2800 cm^{-1} due to C–H stretching vibrations of 1-butene. The highest frequency band is located near 2960 cm^{-1} which is more than 120 cm^{-1} lower than 3086 cm^{-1}

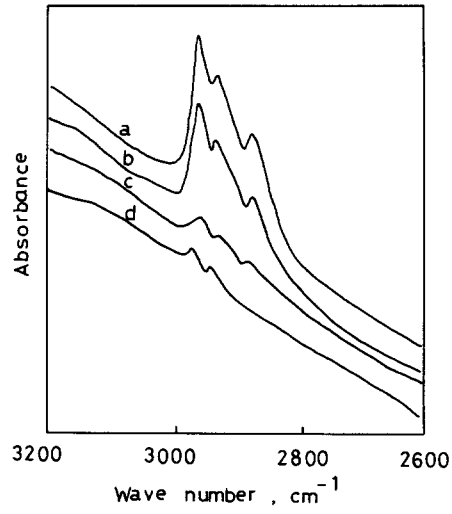

FIG. 5. Infrared spectra (2600–3200 cm^{-1}) of the same sample as in Fig. 2c. The sample was treated in He flow at RT (a), 420 K (b), 520 K (c), and 570 K (d).

for gaseous 1-butene (*6*). However, the position is close to those observed for 1-butene adsorbed on Ni (*7*) or butene oligomers formed on a NaH–Y zeolite (*8*). The intensity of these bands are diminished upon successive heating of the sample. In 1700–1400 cm^{-1} region (Fig. 6), the sample treated at

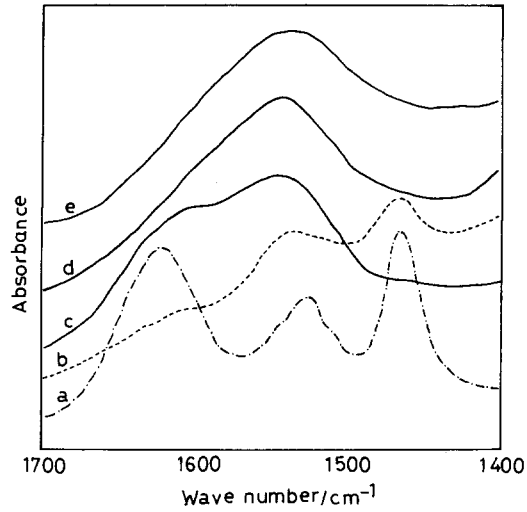

FIG. 6. Infrared spectra (1400–1700 cm^{-1}) of the same sample as in Fig. 2c. The sample was treated in He flow at RT (a), 420 K (b), 520 K (c), 620 K (d), and 720 K (e).

RT exhibits a strong band at 1630 cm^{-1} and two bands at 1530 and 1460 cm^{-1} (Fig. 6a). The first band is due to C=C stretching and the other two are due to CH_3 bending vibrations of 1-butene. Upon heating, these bands disappear and a new broadband appears near 1550 cm^{-1} above 520 K.

Likewise, *n*-butane was adsorbed on a fresh SO_4^{2-}–Fe_2O_3 showing an IR spectrum of Fig. 7a. Following the adsorption of *n*-butane at RT, the characteristic band at 1382 cm^{-1} shifts to 1320 cm^{-1}. Unlike the case of 1-butene, the original IR spectrum of the fresh sample is recovered upon heating of the sample preadsorbed with *n*-butane (Fig. 7e–7f). The IR spectra in Fig. 8 also showed two bands at 2957 and 2926 cm^{-1} following adsorption of *n*-butane at RT due to C–H stretching vibrations. The intensity of these bands diminished greatly upon heating up to 420 K and the bands disappeared at higher temperatures. Most of adsorbed *n*-butane appears to be desorbed at this temperature. The TPDR results also indicated that *n*-butane was completely desorbed below 450 K.

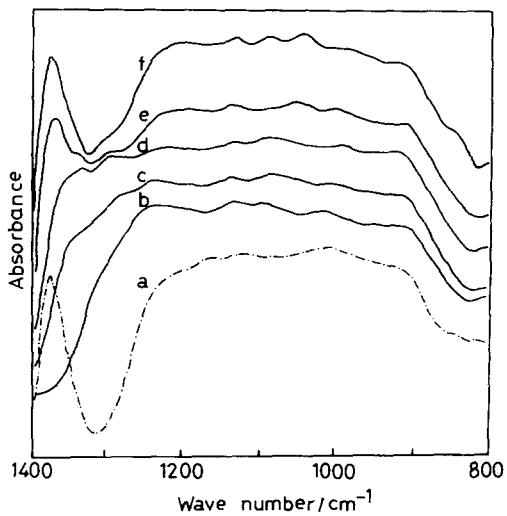

FIG. 7. Infrared spectra (800–1400 cm^{-1}) of SO_4^{2-}–Fe_2O_3 before and after adsorption of *n*-butane. The fresh sample was treated at 760 K for 2h in He flowing at 86 μmol s^{-1} (a). Following adsorption of *n*-butane at RT, the sample was treated at RT (b), 420 K (c), 620 K (d), 670 K (e), and 720 K (f).

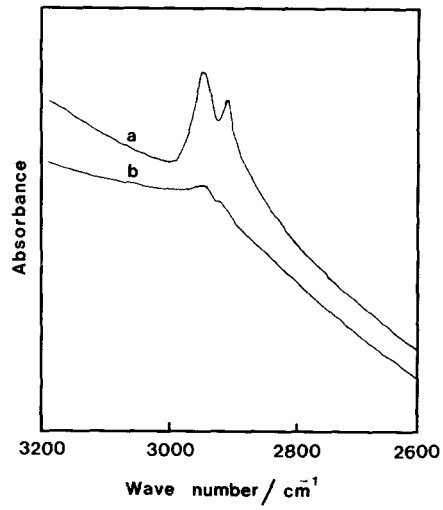

FIG. 8. Infrared spectra (2600–3200 cm^{-1}) of SO_4^{2-}–Fe_2O_3 after adsorption of *n*-butane followed by treatment in flowing He at RT (a) and 420 K (b).

DISCUSSION

Interactions with Adsorbed 1-Butene

The observations made for adsorbed 1-butene are very similar to those for pyridine in our previous study (*3*). Both of them lower the temperature of sulfate decomposition. In TPDR spectra shown in Figs. 2, 3, CO_2, a cross product between SO_4^{2-}–Fe_2O_3 and 1-butene is generated together with the decomposition product SO_2 showing the same peak temperatures and similar peak shapes. This indicates that CO_2 and SO_2 may be produced from a common process and a common intermediate containing C, S, and O. Furthermore, the blank experiments demonstrated that thermal decomposition of SO_4^{2-}–Fe_2O_3 or 1-butene occurs at much higher temperatures. These results suggest that the destabilization by preadsorbed 1-butene is caused by a reaction between sulfate and 1-butene.

The IR data provide more information on the nature of interactions between the sulfate ion and 1-butene. In SO_4^{2-}–Fe_2O_3, the sulfate ion, due to its covalent double bond character, induces the removal of electrons from Fe ion to enhance the Lewis acidity of

the metal ion sites. Upon adsorption of 1-butene at RT on these Lewis acid sites, electrons transfer from the adsorbate to the metal ion, and then to the sulfate ions. The sulfate ion then loses its double bond character and IR band at 1382 cm^{-1} due to S=O shifts to 1310 cm^{-1}. When the sample is heated in He flow, some of adsorbed 1-butene does not simply desorb, but reacts with the sulfate ion to promote its decomposition. Hence the band at 1350 cm^{-1} appears to be due to an intermediate of the decomposition reaction.

Hence the mode of the interaction between adsorbed 1-butene with SO_4^{2-}–Fe_2O_3 can be depicted in the same manner as that in Fig. 1 for pyridine. One interesting aspect of this decomposition of SO_4^{2-}–Fe_2O_3 is that it always removes a surface oxygen leaving an oxygen vacancy behind as shown in Fig. 1 for the species III. The oxygen is removed either as gaseous oxygen as in the case of the sample without preadsorption, or reacts further with hydrocarbon fragments to form CO_2 as in the case of 1-butene and pyridine. The stoichiometry of the decomposition of SO_4^{2-}–Fe_2O_3 with preadsorbed 1-butene appears to be extremely complicated as indicated by complicated TPDR specra and the large number of gaseous products. However, the stoichiometry for the sample without preadsorption seems rather simple:

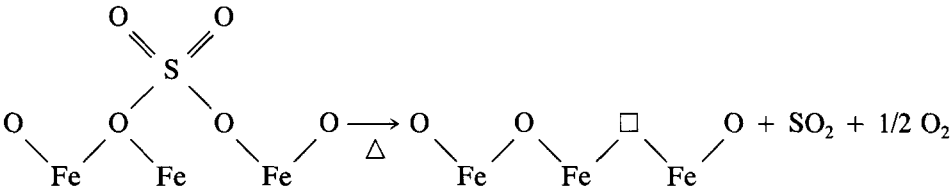

(1)

The □ denotes an oxygen vacancy. Note that the stoichiometry is the reverse of the SO_4^{2-}–Fe_2O_3 formation reaction from SO_2 and O_2 as proposed by Yamaguchi *et al.* (*4*).

In the region of 1700–1400 cm^{-1}, the presence of C=C stretching and CH_3 bending vibrations indicates that 1-butene adsorbs molecularly at RT, probably forming a π-complex (*9*) on SO_4^{2-}–Fe_2O_3. Between 420 and 520 K, original peaks disappear and new broad peaks appear near 1550–1570 cm^{-1}. This behavior of IR bands is very similar to that observed by Kokes and Dent (*9*) for the isomerization of 1-butene on zinc oxide which was shown to proceed through a π-allyl intermediate. The intermediate showed IR bands near 1550–1570 cm^{-1}. Lewis acid sites have been known to be active sites for hydrogen abstraction from olefins to form an allyl species (*10*). Hence, it seems plausible that 1-butene adsorbs on Fe site and forms an allyl species between 420 and 520 K. Another possibility for the bands near 1550–1570 cm^{-1} is due to an oligomeric intermediate of 1-butene which is known to be formed on acidic surface. However, it was reported that there is no IR bands in this region in the surface species formed during 1-butene oligomerization over NaH–Y zeolite or dehydroxylated zeolites (*8*).

Since the band at 1350 cm^{-1} in S=O frequency region appears near the temperature of SO_2 and CO_2 formation, and if the hydrocarbon species observed under the condition is the allyl complex, the following structure IV could be proposed as a possible intermediate of sulfate decomposition.

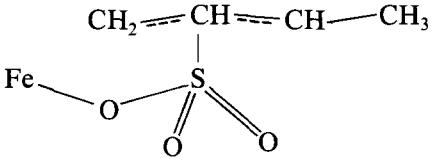

IV

This η^3-allyl species is formally considered to be a three-electron donor as a ligand in organometallic chemistry. The complex is

TABLE 1

Reactions Catalyzed by Sulfate-Promoted Metal Oxides

Reaction	Catalyst	Reaction temp. (K)	Ref.
Double bond isomerization of 1-butene	SO_4^{2-}–Fe_2O_3	373	(*5*)
Skeletal isomerization of *n*-butane or *i*-butane	SO_4^{2-}–Fe_2O_3	273–RT	(*1*)
	SO_4^{2-}–ZrO_2	373–523	(*13*)
	SO_4^{2-}–TiO_2	323	(*14*)
Esterification of terephthalic acid	SO_4^{2-}–TiO_2	473	(*2*)
Acylation of chlorobenzene with benzoyl chloride	SO_4^{2-}–ZrO_2	408	(*2*)
Ring-opening isomerization of cyclopropane	SO_4^{2-}–Fe_2O_3	373–423	(*5, 15*)
Dehydration of 2-butanol	SO_4^{2-}–Fe_2O_3	373–423	(*5*)
Dehydration of 2-propanol	SO_4^{2-}–Fe_2O_3	473	(*15*)
Liquefaction of coal	SO_4^{2-}–Fe_2O_3	673	(*2*)
Methane-ethylene coupling	SO_4^{2-}–ZrO_2	573	(*16*)
Methanol to hydrocarbons	SO_4^{2-}–$ZrO_2Al_2O_3$	553–573	(*17*)
Dehydrocyclization of hexane to benzene	SO_4^{2-}–ZrO_2	823	(*18*)

analogous to species III of Fig. 1 which was proposed in the case of the pyridine and SO_4^{2-}–Fe_2O_3 system (*3*). Hence, both nitrogen in the cases of pyridine and ammonia and the π-allyl species for 1-butene appear to serve as electron donors to form proposed complexes. The formation of these species weakens the S=O bond of SO_4^{2-} as evidenced by the shift of IR band to lower frequencies. The migration of adsorbates from metal to sulfur is reminiscent of the migration, due to heating, of an alkyl group within the coordination sphere of rhodium carbonyl dithiolates from acyl ligand through Rh to a coordinated sulfur (*11*).

Interactions with Adsorbed n-Butane

n-Butane adsorbs on SO_4^{2-}–Fe_2O_3 at RT as indicated by IR results. Since this type of catalyst is known to isomerize *n*-butane at RT (*1*), this adsorption could be a pathway to the reaction. The adsorption appears to be weak since most of adsorbed *n*-butane was desorbed upon heating above 450 K. Because of this early desorption, it is not surprising that S=O recovers its original IR band position upon heating above 670 K. The difference between the temperature of *n*-butane desorption and that at which the sulfate band is restored is believed to be due to the presence of water introduced inadvertently into the system when *n*-butane was adsorbed. In contrast to the case of 1-butene, the presence of water was noted by IR for the sample adsorbed with *n*-butane. As discussed elsewhere (*3*), water adsorbed on Fe site of SO_4^{2-}–Fe_2O_3 would not influence the stability of the sulfate group. However, it should have hindered adsorption of *n*-butane by occupying the Lewis acid site which appears to be the adsorption site of *n*-butane as well. Also it affects IR spectra of the sulfate group. In any case, by the time the sample reaches the temperature at which the sulfate group could react, there is no *n*-butane in the system. This negligible effect of *n*-butane on the stability of SO_4^{2-}–Fe_2O_3 is similar to that observed for ammonia (*3*). However, the behavior of *n*-butane should be differentiated from that of ammonia whose interactions with the sulfate are insignificant even when it is present in the system. On the other hand, *n*-butane, if present in the gas phase during catalytic reactions, may react with the sulfate ion above 450 K and, thus, destabilize the catalyst. Indeed, the sulfate started to decompose at 570 K

when gaseous *n*-butane was introduced during TPDR.

Implications in Catalysis by SO_4^{2-}–Fe_2O_3

In catalysis by sulfate-promoted metal oxide catalysts, it has been assumed that the sulfate group induces the removal of electrons from the metal ion to enhance the Lewis acidity of the metal ion site, and does not interact directly with reactants (*12*). Hence, the temperature of their thermal decomposition has been regarded as the highest temperature at which these catalysts could be used without serious degradation. The results of the present study demonstrate that the spectator's role of the sulfate group is true only below the temperature at which the reactants begin to react with sulfate and remove it from the catalyst surface. This temperature of chemical decomposition, rather than the temperature of thermal decomposition, should be considered as the upper limit of application of sulfate-promoted metal oxide catalysts. In the present study, we considered interactions with adsorbed species only. Under the condition of catalytic reactions, however, the presence of reactant in the gas phase may contribute further to accelerated degradation of the sulfate ions. Hence, as mentioned, molecules such as *n*-butane which were found to be innocuous under the conditions of the present study may still destabilize the catalyst significantly during catalytic reactions. Table 1 lists typical reactions studied over these catalysts and their reaction temperature (*1, 2, 5, 12–18*). None of the studies report on the stability of the catalyst. However, it appears that some reactions were run at temperatures at which degradation might have occurred due to interactions between reactants and the sulfate ion.

A recent review (*19*) discusses potential causes of deactivation of sulfate-promoted metal oxide catalysts. As usually observed for strong acid catalysts, coke formation could be a cause of the loss in catalytic activity. When a reaction is carried out in a reducing atmosphere, the catalysts were shown to deteriorate by reduction of S^{+6} to an inactive sulfur species, and migration of sulfur into the bulk of metal oxides. The loss by sulfur reduction could be completely restored by reoxidation as demonstrated by Yori *et al.* (*20*) in *n*-butane isomerization at 573 K over SO_4^{2-}–ZrO_2. On the other hand, migration into the bulk caused a permanent loss of activity. In the light of the present work, a new route to deactivation of these catalysts by chemical decomposition of sulfate group must be added to the above list.

ACKNOWLEDGMENT

This work has been partly supported by the Korean Science and Engineering Foundation (K72320).

REFERENCES

1. Hino, H., and Arata, K., *Chem. Lett.*, 1259 (1979).
2. Tanabe, K., "Heterogeneous Catalysis" (B. L. Shapiro, Ed.), p. 71. Texas A&M Univ. Press, College Station, TX, 1984.
3. Lee, J. S., and Park, D. S., *J. Catal.* **120,** 46 (1989).
4. Yamaguchi, T., Jin, T., and Tanabe, K., *J. Phys. Chem.* **90,** 3148 (1986).
5. Tanabe, K., Kayo, A., and Yamaguchi, T., *J. Chem. Soc. Chem. Commun.*, 602 (1981).
6. Sheppard, N., and Simpson, D. M., *Quart. Rev. Chem. Soc.* **6,** 1 (1962).
7. Eischens, R. P., and Pliskin, W. A., *Adv. Catal.* **10,** 1 (1958).
8. Dakta, J., *Zeolites* **1,** 113 (1981).
9. Kokes, R. J., and Dent, A. C., *Adv. Catal.* **22,** 1 (1970).
10. Gates, B. C., Katzer, J. R., and Schuit, G. C. A., "Chemistry of Catalytic Processes." p. 15. McGraw–Hill, New York, 1979.
11. Cheng, C.-H., and Eisenberg, R., *Inorg. Chem.* **18,** 2438 (1979).
12. Jin, T., Yamaguchi, T., and Tanabe, K., *J. Phys. Chem.* **90,** 4794 (1986).
13. Hino, M., and Arata, K., *J. Amer. Chem. Soc.* **101,** 6439 (1979).
14. Hino, M., and Arata, K., *J. Chem. Soc. Chem. Commun.*, 1148 (1981).
15. Nagase, Y., Jin, T., Hattori, H., Yamaguchi, T., and Tanabe, K., *Bull. Chem. Soc. Japan* **58,** 916 (1985).

16. Scurrel, M. S., *Appl. Catal.* **34,** 109 (1987).
17. Yamamoto, M., Yoshida, T., and Kotanigawa, T., *J. Chem. Soc. Japan* **5,** 838 (1985).
18. Hino, M. and Arata, K., *Chem. Lett.,* 1483 (1985).
19. Tanabe, K. and Yamaguchi, T., "Successful Design of Catalysts" (T. Inui, Ed.), p. 99. Elsevier, Amsterdam, 1989.
20. Yori, J. C., Luy, J. C., and Parera, J. M., *Appl. Catal.* **46,** 103 (1989).